10th IMC
10th International Masonry Conference
G. Milani, A. Taliercio and S. Garrity (eds.)
Milan, Italy, July 9-11, 2018

A STRUCTURAL PARADOX IN THE CHURCH OF THE NATIVITY: FE STATIC ANALYSES

Claudio Alessandri[1], Matteo Del Balzo[2], Gabriele Milani[2], and MarcoValente[2]

[1] Department of Engineering, University of Ferrara
via Saragat 1, 44100 Ferrara, Italy
e-mail: claudio.alessandri@unife.it

[2] Department of Architecture, Built environment and Construction engineering ABC, Technical University of Milan
Piazza Leonardo da Vinci 32, 20133 Milan, Italy
e-mail: {gabriele.milani, matteo.delbalzo, marco.valente}@polimi.it

Keywords: masonry church, collapse of a column, vertical loads, static non-linear analyses, arches.

Abstract. *The colonnades of the Church of the Nativity in Bethlehem are topped by wooden architraves above which the masonry walls of nave and transept were erected. During the archaeologic campaign carried out in the Thirties of the last century the presence of relieving arches was discovered between the architraves and the walls, hidden for centuries under thick layers of plaster and walls mosaics. Each arch covers the span between two columns and rests on the underlying architrave without any direct link other than that provided by friction at the interface. This peculiar construction system caused over time a crush of the most compressed parts of the architraves and was thought as one of the possible causes of some cracks now visible in the central column of each corner. Here the resultant of the horizontal components of the two thrusts coming from the two arches of the corner should be transferred to the architraves by friction, as no particular connection, like nails or iron rods, was found between masonry and architraves. But, the standard friction coefficient between wood and masonry is not enough to ensure this interaction at the interface and, according to the approximate calculations made with linear elastic models, an overturning of the central columns and of the structure above should occur. Nevertheless, despite some weakness planes surveyed in these columns, there are no signs of incipient collapse and both corners seem to be quite stable. The aim of this paper is to use appropriate numerical simulations to create different scenarios that might justify the present static situation. The numerical analyses will take into account the nonlinear behavior of masonry, the orthotropic behavior of the wooden architraves and the unilateral contact between masonry walls and architraves.*

Peer-review under responsibility of the organizing committee of 10th ICM.

1 INTRODUCTION

According to the most recent studies [1], the Church of the Nativity was completely re-built upon the remains of Constantine's previous Church (5th century AD) in the 6th century AD by Emperor Justinian. Its longitudinal body, which is slightly longer than the previous footprint (see Figure 1a), consists of a nave with four flanking aisles and four colonnades, two on each side. A transept and an apse took the place of the original octagonal structure built above the main Grotto, which was visible from a hole placed in the center of the octagon.

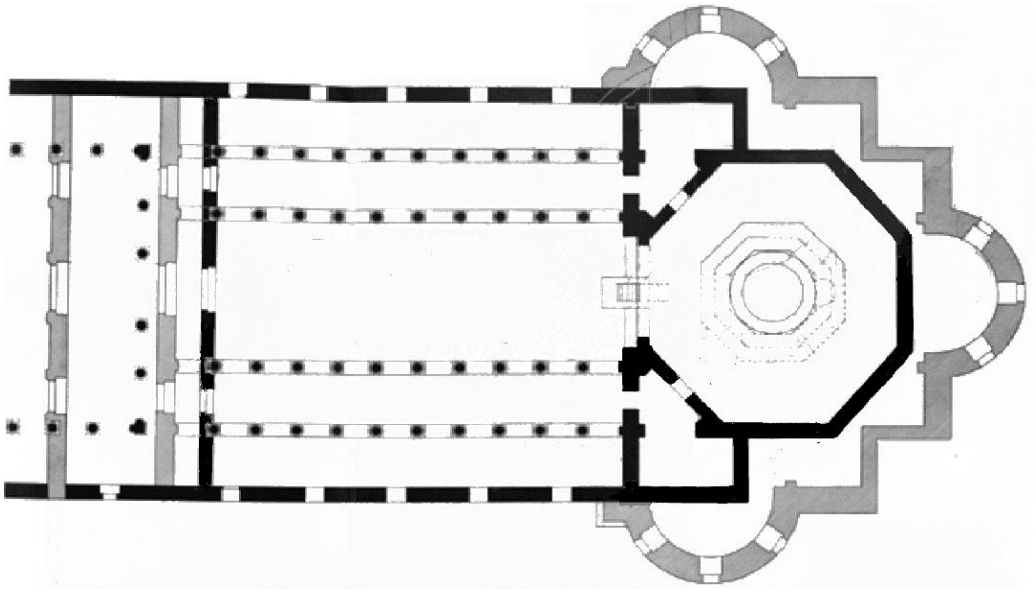

(a)

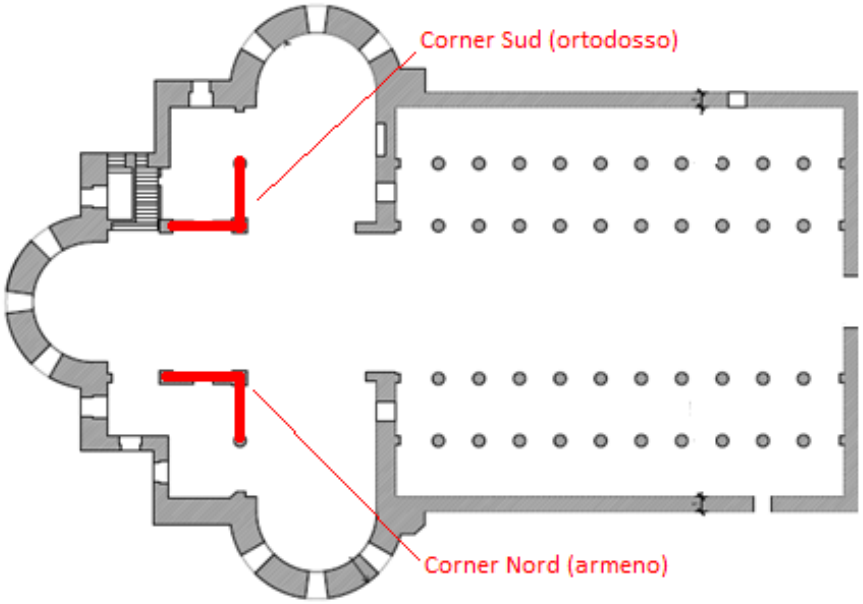

(b)

Figure 1: (a) The Basilica according to Bagatti's re-construction. Black: Constantine's Church. Grey: Justinian's Church. (b) The Justinian church with the North and South corners.

Therefore, the basilica has the classic Latin cross plan of the Christian churches, with the main body approximately 64 m long and 40 m wide and its longitudinal axis placed in the West-East direction, according to the Byzantine tradition (see Figure 1b). Detailed archaeo-

logical reports can be found in the books of Hamilton [2] and Harvey [3], as well as in the comprehensive research carried out over many years by Bagatti [4].

As shown in in Figure 2, the roof structure consists of two distinct types of trusses: those supporting the roof of nave and transept, and those supporting the roof of aisles and corners, the letter placed at the intersection of nave and transept.

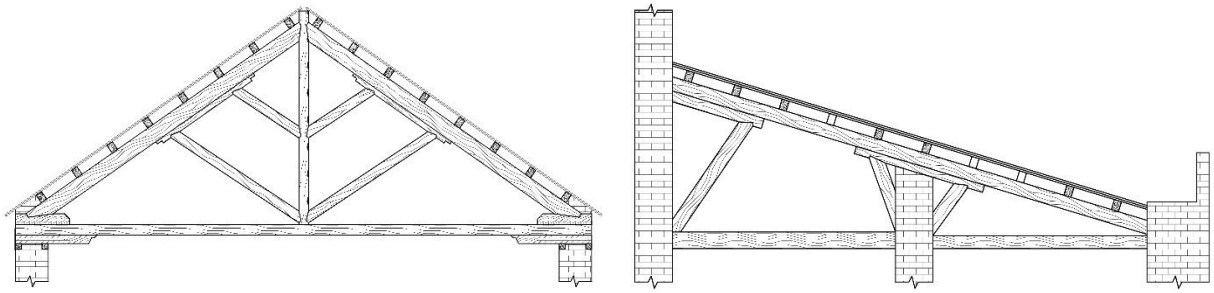

(a) (b)

Figure 2: Trusses of nave and transept (a) and aisles and corners (b).

Wooden architraves are placed above the four colonnades of the nave and the aisles and above the columns of the corners. Made of Lebanese cedar, they were introduced as tie-beams whose basic purpose was to connect the columns together and to absorb the horizontal thrust components at both ends of each colonnade [5]. Each of them consists of three beams set side by side and extends over three successive spans. It must be noted that the weight of the upper walls is borne not by the wooden architraves, yet by arcades, or more specifically by low, relieving arches, springing from the architraves themselves (Figure 3). The space between the intrados of the arch and the extrados of the architrave is filled with stones. The entire masonry is then covered with a layer of plaster or wall mosaics.

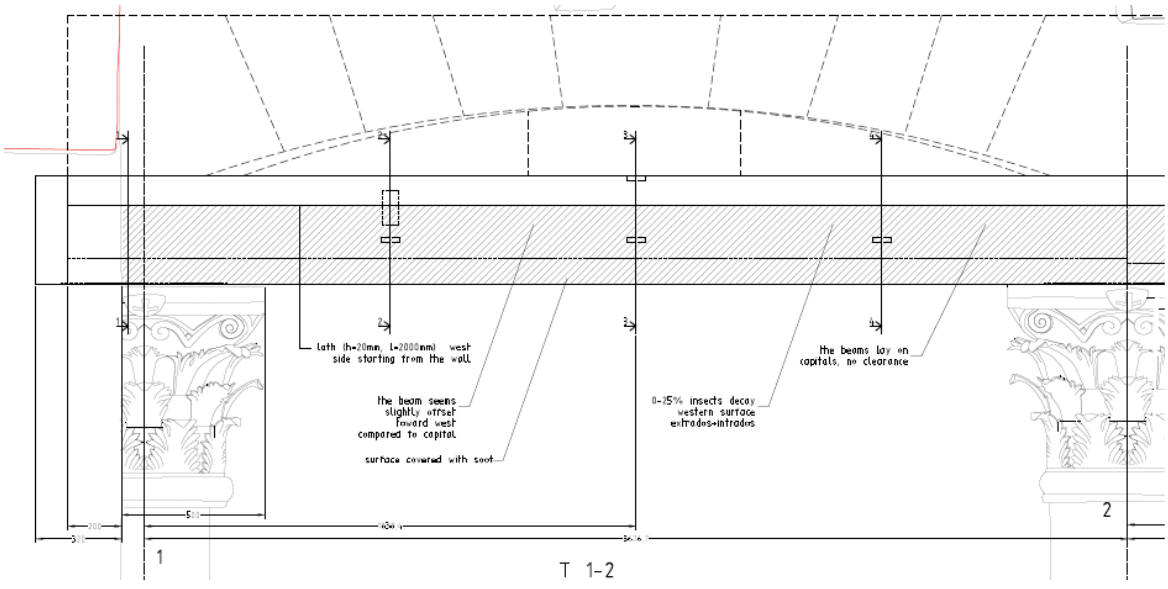

Figure 3: Relieving arches above architraves.

The state of decay, surveyed during the restoration works of the whole Church, started in 2012 on the basis of a previous diagnostic campaign [6][7], was various and diversified: some parts were missing, there were cracks, incoherent deposits, material deterioration due to fungi and insect attacks, spots due to water percolation. The state of decay worsened also in conse-

quence of unsuitable interventions made in the past, like painting of capitals and wooden surfaces, some inappropriate superficial treatments and also in consequence of human negligence that produced visible anthropic damages. The two corners are symmetrical with respect to the longitudinal axis of the church and differ only for some details that are negligible from a structural point of view.

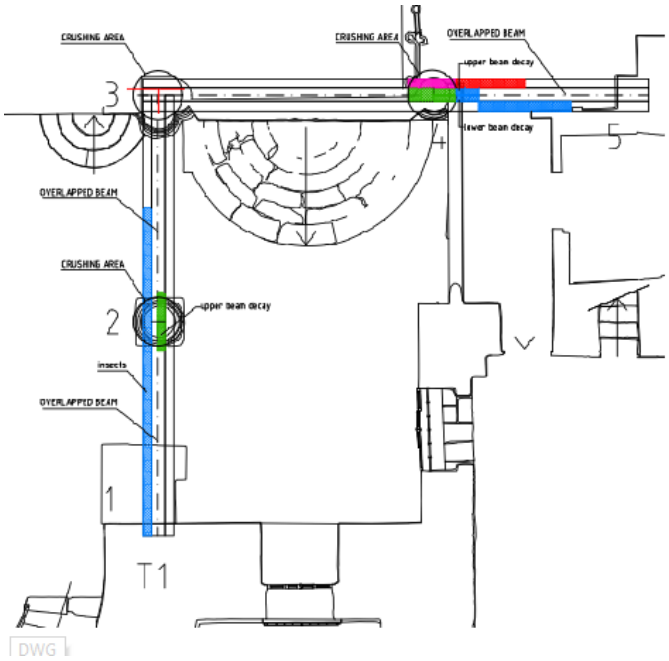

Figure 4: South (Orthodox) corner.

As shown in Figure 4, the corner is made up of 5 marble columns, 5.5 m high, topped by wooden architraves. As mentioned previously, relieving arches springing directly from the architraves and with a span equal to the distance between the columns, support the walls of the basilica, which are 8,60 m high. These walls contained four windows (Figure 5), some of which were buffered probably after the seismic events occurred in the first half of the 19th century.

Figure 5: Walls of the corners.

In particular, the investigations carried out in the architraves of the Orthodox and Armenian corners, so called after the 1852 status *quo* that placed them under the direct control of the Orthodox (South corner) and Armenian (North corner) Communities (which run the church along with the Custody of the Holy Land), highlighted a structural problem already envisaged

in 1932 by Harvey during his archaeological campaign [3]. In fact, the central columns of both corners, in correspondence of the intersection of the nave and transept walls, show some weakness planes differently oriented, which have always raised concerns since their first detection at the beginning of the last century. The last restoration works carried out in the church, in particular in the architraves of the corners, offered the opportunity to analyze in detail such a problem.

It was thought that these weakness planes (it is not clear yet if they correspond to actual cracks) could be the consequence of high thrusts transferred from the relieving arches to the lintels and from these to the capitals of the columns through the friction between masonry arch and wooden lintel and between wooden lintel and stone capital. It is worth noting that before the restorations the lintels were seriously damaged and had lost, even though partially, their ability to work as tie-beams. From initial, approximate analyses carried out by assuming material linear elastic behaviors, the magnitude of the resultant horizontal component of the thrust coming from the two corner arches resulted to be so high that it could not be absorbed by friction alone. It was therefore thought of a possible interpenetration of the masonry in the lintel, such as to constitute an effective constraint to the sliding of the masonry on the architrave, but a more accurate survey of the interface masonry-lintel excluded the existence of any interpenetration. Moreover, there were no signs of damage on the walls, such as to denounce a mechanism of collapse and, even if there had been in the past, they had been covered over the centuries by thick layers of plaster and by the wall mosaics. Nevertheless, despite these concerns and doubts about their stability, the corners seemed not to suffer any harmful effect. It was therefore considered that an explanation of the current state and a more complete and exhaustive answer to the doubts arisen so far could be provided by a more accurate analysis to be carried out with more appropriate tools, able to tackle the problem in all its complexity.

The purpose of this paper is to verify the present static condition of both corners through a series of structural analyses based on the finite element method (FEM). Such analyses will concern the overall behavior of the corners, studied by means of homogeneous and heterogeneous models, and the local behavior of some structural elements, judged to be more at risk, such as the relieving arches and the central column.

2 MATERIAL CHARACTERISTICS

The definition of the mechanical behavior of masonry depends on the mechanical parameters of blocks and mortar, but also from a series of factors related to the construction methods of the masonry itself. A numerical estimate of the mechanical parameters can be obtained by in situ experimental tests or by the method based on the Masonry Quality Index (*IQM*) [8].

It should be noted that the values of the material characteristics of the masonry walls of both corners are assumed equal to the ones obtained, during the restoration works [9], with the *IQM* method for the masonry wall in common between narthex and naves. In fact, these walls show the same morphological and material characteristics, i.e. size of the blocks, state of conservation, quality of the mortar joints, etc.

According to [8] where the meaning of the symbols used is clearly explained, the relation:

$$IQM_v = REEL_V\,(OR_V + PD_V + FEL_V + SG_V + DEL_V + MA_V) \tag{1}$$

provides an Index value IQM_V = 8.5. Since this value is between 0 and 10, it can be stated that the quality of this particular masonry quite good. The *IQM* method allows to correlate the *IQM* value, related to vertical loads, with the value of the compressive strength of the masonry and with the Elastic Modulus, as shown in Table 1 obtained by using Table C8A.2.1 of Circular 617/2009 [10].

	MIN	MED	MAX
f_m [MPa]	6.29	7.74	9.19
E [MPa]	2411	2858	3305

Table 1: maximum, average, minimum mechanical parameters.

Moreover, according to the Italian norms NTC2008 [11] for the lowest level of knowledge (LV1), the minimum resistance value and the average value for the elastic modulus must be considered. It is also stated that, for the latter, a reduction of 50% has to be applied in order to consider the occurrence of possible cracks. With reference to Table C8A.2.1 of [11] it is also possible to obtain the value of the Shear strength and of the Shear module to which the same requirements are also applied, i.e. minimum value for resistance, average value reduced by 50% for the Shear module. Ultimately, the mechanical parameters that characterize the masonry are those summarized in Table 2.

f_m [MPa]	**E [MPa]**	**τ_0 [MPa]**	**G [MPa]**
6.29	1429	0.12	389

Table 2: mechanical parameters used.

3 MATERIAL MODELLING

The non-linear behavior of masonry was described by means of the Concrete Damage Plasticity (CDP) model available in the ABAQUS/Standard materials library [12]. This model was primarily intended for the analysis of concrete structures under cyclic and dynamic loading [13][14], but it has been widely shown that it can be also adapted to masonry/stones/mortar. Recent numerical examples of application to historical masonry structures can be found in e.g. [15]-[22]. The CDP model is a continuum plasticity based damage model in which the main failure mechanisms are tensile cracking and compressive crushing. The model is able to assign different strengths, stiffness degradation and recovery effect terms both in tension and compression, as schematically shown in Figure 6.

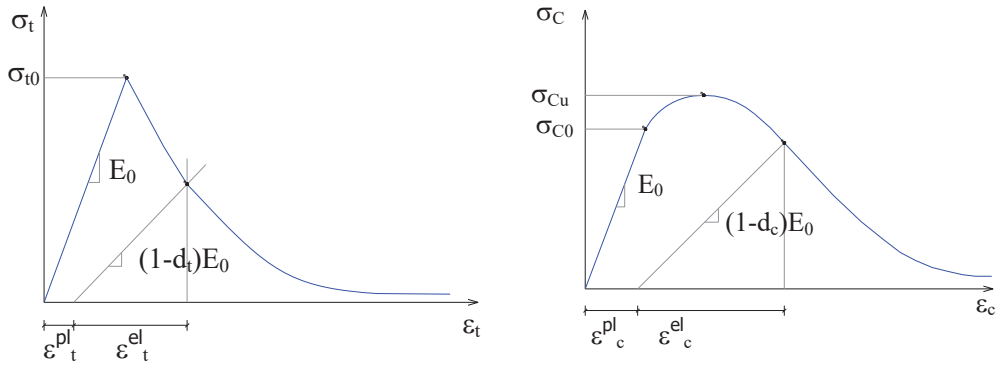

(a) (b)

Figure 6: Mechanical behavior of masonry under uniaxial (a) tension and (b) compression.

To define the CDP model in Abaqus, the values of the following parameters are adopted for masonry/stones/mortar: 1) the dilation angle is assumed equal to 10°, in agreement with experimental data available in the literature, see for instance [15]; 2) the flow potential eccentricity is set equal to 0.1, as suggested by the user's Guide [12]; 3) the ratio of initial biaxial

compressive yield stress to initial uniaxial compressive yield stress is equal to 1.16, in agreement with numerical and experimental results reported in e.g. [23]; 4) the ratio of the second stress invariant on the tensile meridian to that on the compressive meridian is set equal to 0.666, as suggested by the user's Guide [12]; 5) the viscosity parameter, which defines viscoplastic regularization, is assumed equal to 0.002.

4 NUMERICAL MODELLING

Both corners were modeled by using homogeneous and heterogeneous approaches. In the first one, easier to handle, masonry is modeled as a continuous nonlinear material and the wooden architraves as linear elastic material; in the latter a distinction is made between stones and mortar joints, whereas the wooden lintels are modeled in the same way. The choice of a homogeneous model is due to the necessity to have some reference data, though approximate, to be compared with those of the heterogeneous, more realistic model, which can take into account the interactions among stones, the constructive features of the arches, the way in which windows were buffered, all issues that influence the actual behavior of the corners and that in no way could they be taken into account in a homogeneous model. Geometry, loads and boundary conditions are the same for both models in order to have comparable results.

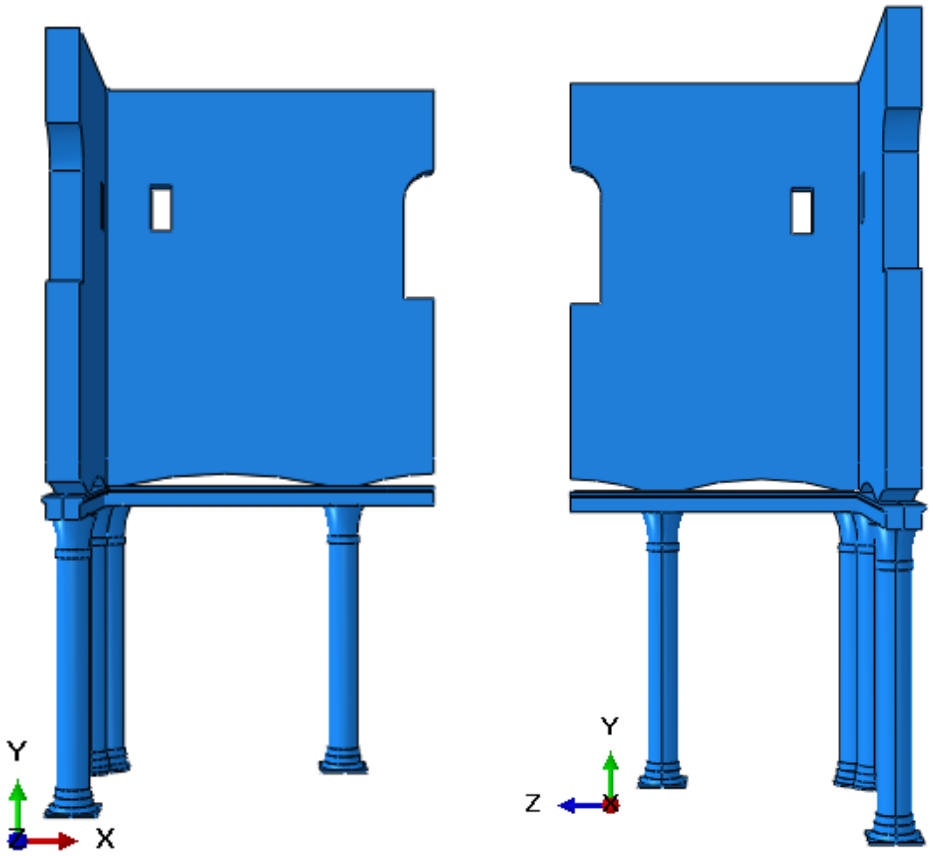

Figure 7: Homogeneous model – lateral views.

4.1 Homogeneous model

The geometrical model is generated by Abaqus and consists of that part of the corner including one arch and a half on each side, three columns one of which at the intersection of nave and transept, architraves and walls with the existing openings, see Figure 7. The filling

between arches and lintels has not been considered because made of scarcely consistent material. Moreover, the bases of the columns are clamped and symmetry in X and Y directions is considered, with X and Y parallel to nave and transept respectively. The arches are simply supported by the lintels, as well as the lintels are simply supported by the columns. Therefore, each component can slide on the other and the interaction at the interface is defined on the basis of suitable values of the static and dynamic friction coefficients. The load conditions are defined with reference to the composition of the roof covering existing before the its replacement with a new roof covering. In this analysis only the self-weight of masonry walls and roof covering is considered. These loads will be incremented by apposite multipliers in order to evaluate the mechanical behaviour of the whole structure under these increasing loads up to the final collapse. Wind and snow have not been considered. The values of such loads were computed with reference to the technical literature and to data provided by the onsite survey. The material components of the roof covering are summarized in Table 3.

Material	**Load Density**
Secondary structure (purlins)	0.27 kN/m^2
Wooden boards	0.12 kN/m^2
Lead sheets	0.23 kN/m^2
Bitumen layer	0.10 kN/m^2
Total	**0.72 kN/m^2**

Table 3: Load density of the material components of the roof covering.

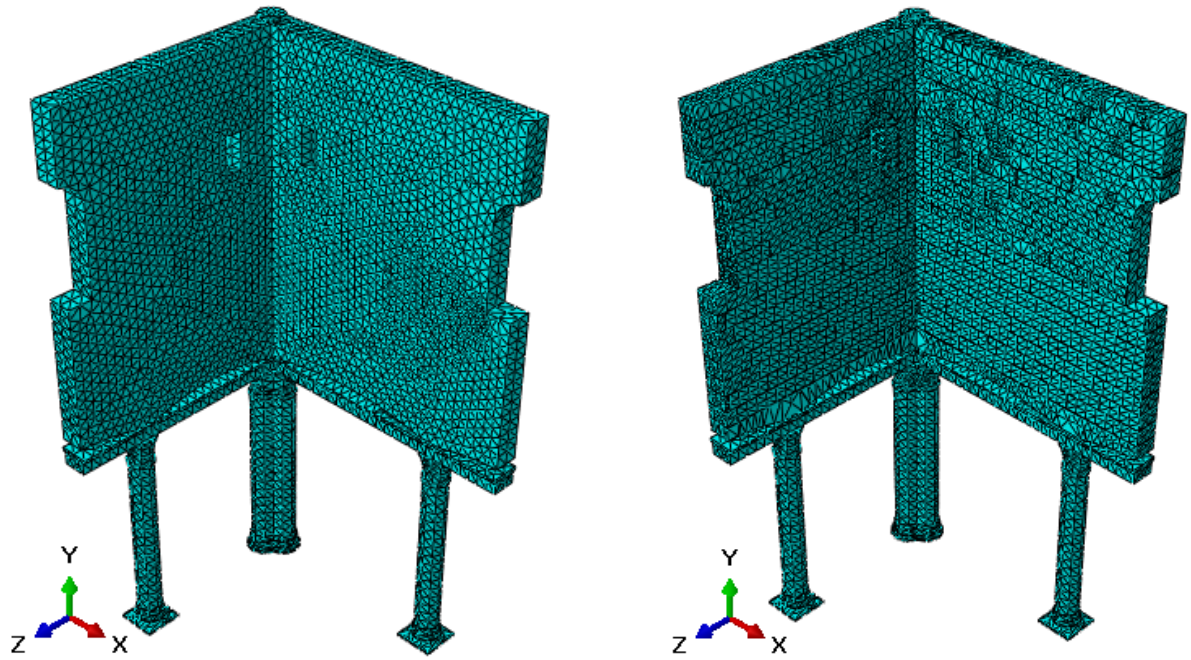

(a) (b)

Figure 8: Discretized homogeneous (a) and heterogeneous (b) model.

Therefore, the following loads are defined above the walls: (i) loads on the walls of the nave equal to 15.83 kN/m^2 and (ii) loads on the walls of the transept equal to 11.53 kN/m^2.

These values include the loads of two roofs, the one of the nave and the one of the roof supported by the half trusses, placed at a lower level and covering the L spaces in the corner between nave and transept. However, for the sake of simplicity, all these loads were applied to the top of the walls. The model is discretised with 403 nodes and 47160 C3D4 elements, i.e. 4 nodes linear tetrahedrons, as shown in Figure 8a.

4.2 Heterogeneous model

It differs from the homogeneous one only for the distinction between stones and mortar joints. The joints are modelled with 3-D elements, 1cm thick, although the actual joints have a smaller thickness. The assembly of the stones is consistent with the data of the survey. Where the walls are covered either by plaster or by mosaics an assembly of stones was hypothesized with vertical joints staggered by 15 cm in order to assume the most unfavourable configuration. Also the stones of the relieving arches were faithfully reproduced (Figure 9). The columns were modelled as unique blocks of marble as they are in reality. The lintels are the same as in the homogeneous model. Although the same *Concrete Damage Plasticity* material model is used, it was necessary to modify the strength characteristics in order to simulate the different mechanical behaviour of mortar and stone and obtain more realistic diagrams for the plastic behaviour in tension and compression. In fact, the values used for masonry in the previous Section, correspond to an intermediate behaviour between the one of the stone and the one of the mortar. The material characteristics of the stones and mortar are shown in Table 4.

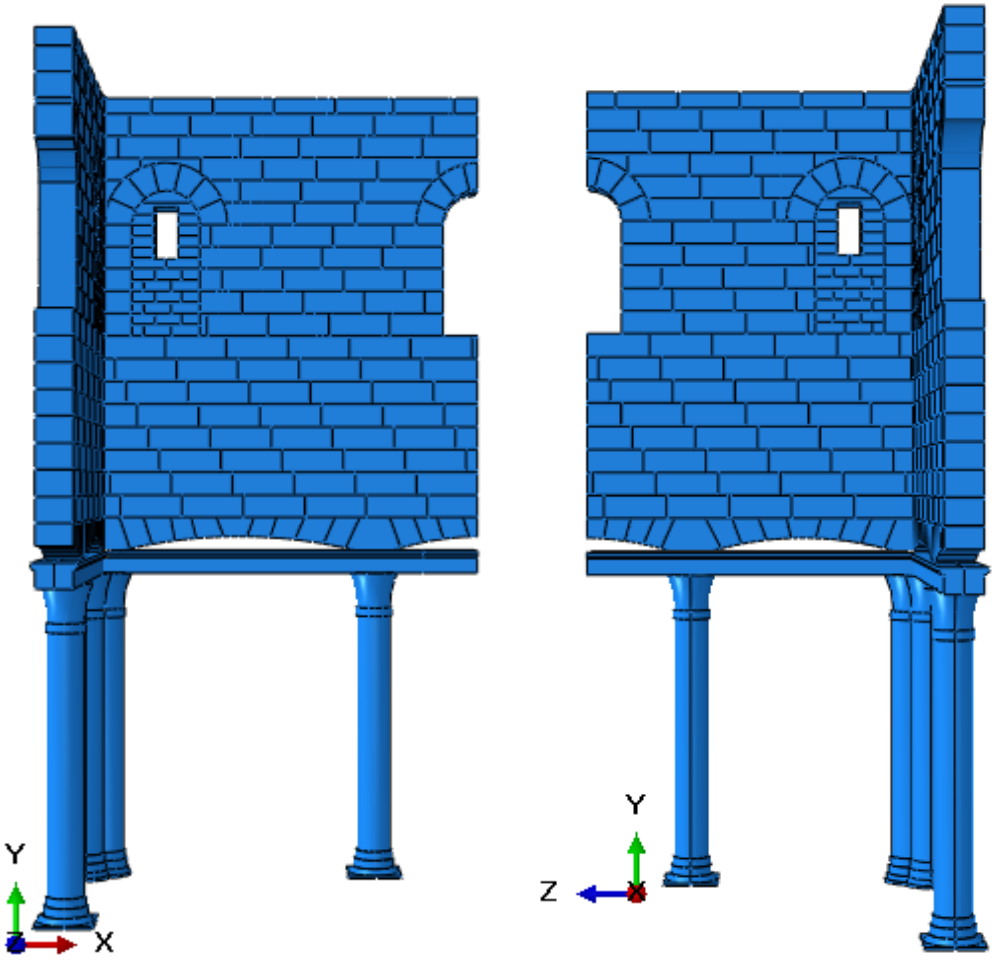

Figure 9: Heterogeneous model – lateral views.

It is with noting that the value of the Elastic Modulus was incremented in order to take into account the greater stiffness of the stone compared with the one of the mortar.

Loads, boundary and interface conditions are the same as in the homogeneous model. The mesh used for discretization (Figure 8b) consists of 34281 nodes, 81895 tetrahedrons most of which are of C3D4 type. Because of the high complexity of the model, also some elements with 10 nodes – C3D10 type, were used. The characteristic dimension of the elements in the stones is 20 cm; in the mortar joints this dimension is 5 cm in order to avoid excessive distortions.

	f_m [MPa]	E [MPa]	τ_0 [MPa]
Stones	10.31	1929	0.18
Mortar	1	1430	0.12

Table 4: Material characteristics of stones and mortar.

5 NUMERICA RESULTS

Both models were tested with the same load and boundary conditions in order to define possible differences in terms of results. These are mostly comparable in columns and lintels, which are modeled in the same way in both cases. In the walls the stresses in the horizontal directions X and Z are quite comparable, although with a more articulated distribution in the heterogeneous model. On the contrary, the vertical stresses, indicated by Abaqus with S22, differ considerably. In the compressed areas, these stress values are much greater in the heterogeneous model. Moreover, always in this model, it is possible to distinguish very clearly some areas with greater stiffness, corresponding to some structural elements such as the arches of the buffered windows and the relieving arches above the lintels (Figure 10). In no way could they be identified by the homogeneous model.

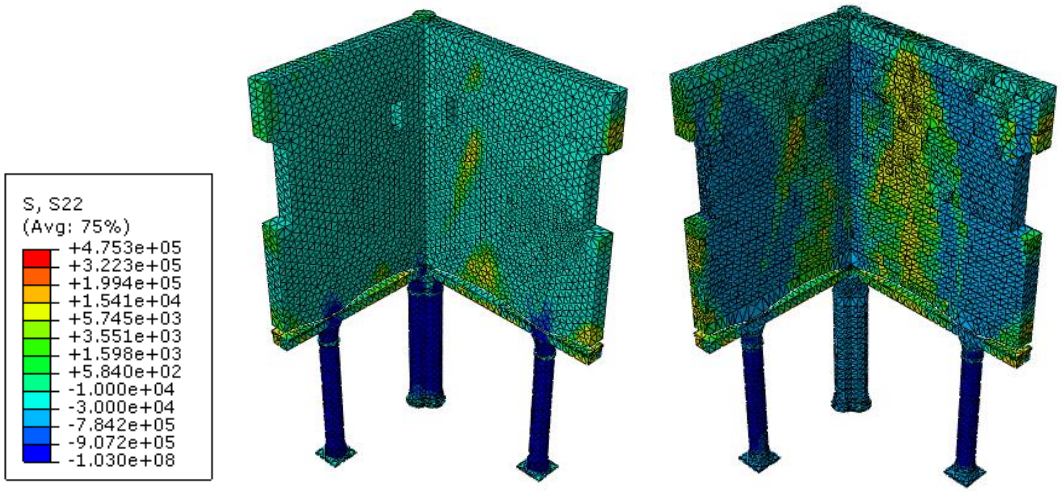

Figure 10: Vertical stresses in the homogeneous (left) and heterogeneous (right) model.

Great differences can be noted between the two models also in terms of damage due to tension, highlighted by the so-called Damage Index in Tension (DAMAGET), see Figure 11. In the homogeneous model there are very few damaged areas whereas in the heterogeneous one clear damage zones develop in almost vertical directions starting from the most stressed areas of the relieving arches and following the trend of the vertical joints. Instead, in both models the displacement values are so small as to make any comparison meaningless. Therefore, the

greater level of detail of the results obtained with the heterogeneous model makes this model more suitable to analyse the mechanical behaviour of the corners.

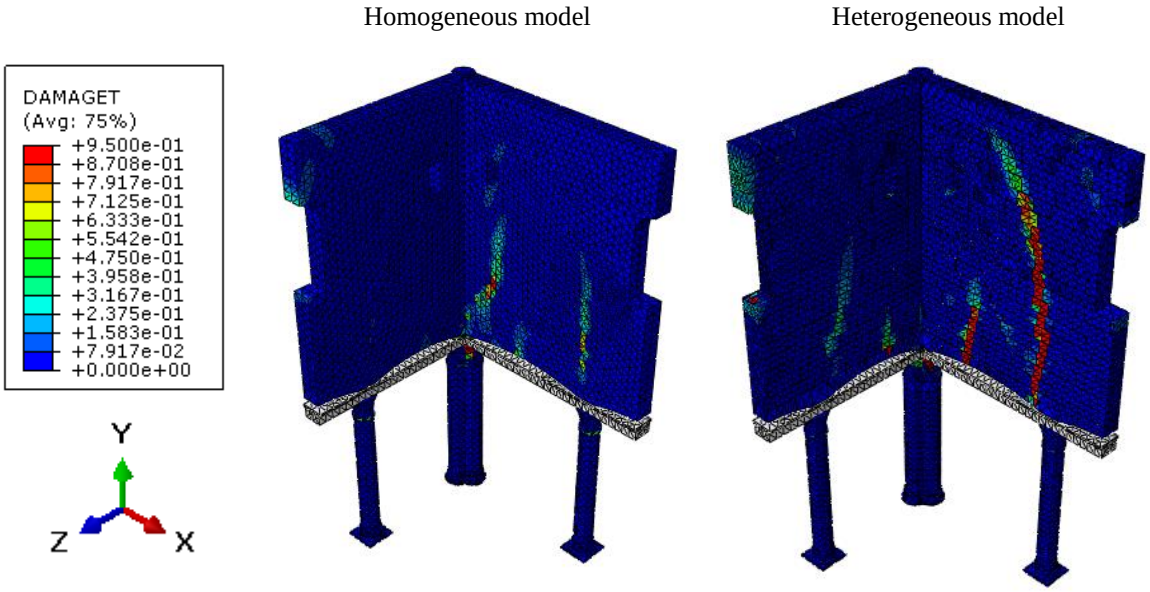

Figure 11: South Damage Index in homogeneous and heterogeneous model.

The numerical analyses on the heterogeneous model were carried out with three different load conditions starting from the one defined in the previous Section and assumed as basic load condition. The other two, obtained from the first one by using multipliers 2 and 4, are useful to understand the evolution of the damage process as the loads are increased up to values corresponding to the final collapse. The incremented values of the loads are so high that they can include also the loads due to snow and wind, that had not been considered in the basic load condition. They can also compensate for any mistake that might have been made in the evaluation of the actual self-weights of wood and masonry.

Even the static and dynamic friction coefficients between lintels and stones, μ_s and μ_d respectively, vary between basic values provided by the technical literature and infinite values corresponding to a possible state of interpenetration of the masonry in the lintel or of the capital in the lintel. Table 5 and Table 6 contain the load and friction values that have been used.

Analyses	**Load density nave direction [kN/m^2]**	**Load density transept direction [kN/m^2]**
1st (basic loads)	15.83	11.53
2nd (multiplied by 2)	31.66	23.06
3rd (multiplied by 4)	63.32	46.12

Table 5: Analyses corresponding to different load conditions.

5.1 Thrust components in the arches

First of all, the vertical and horizontal components of the thrusts exerted by the two arches on the central column of each corner are computed under constant basic friction coefficients and increasing loads. In particular, as shown in Figure 12 and Figure 13, Fx denotes the horizontal component in the nave direction X, Fz the horizontal component in the transept direction Z and Fy the vertical component along the axis of the central column. This analysis

allows to evaluate how the results in terms of thrust change as the loads increase with the same basic coefficients.

Analyses	μ_s [-]	μ_d [-]
1b	0.7	0.3
2b	0.9	0.6
3b	1.2	0.9
4b	2	1.8
5b	∞	∞

Table 6: Analyses corresponding to different friction coefficients.

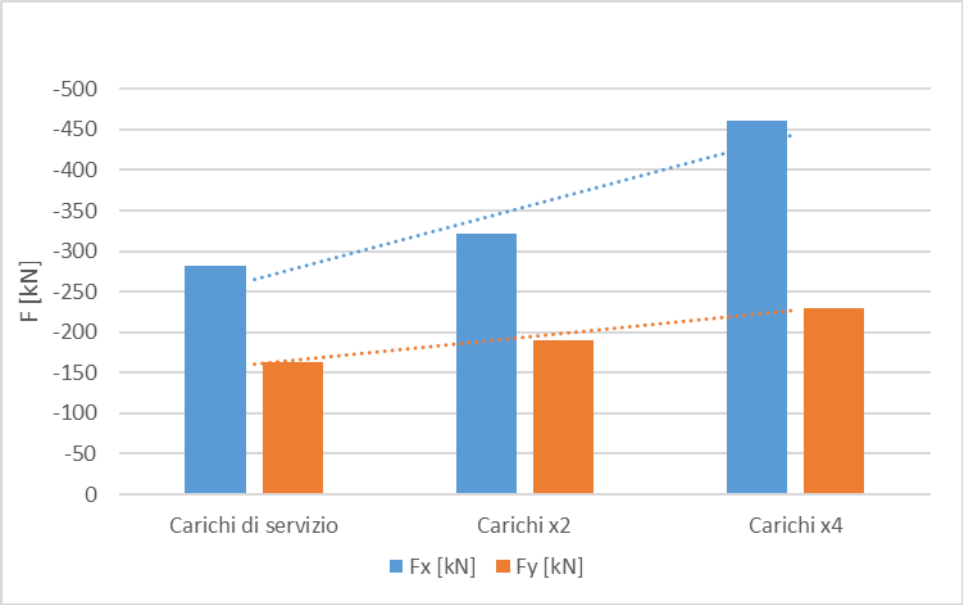

Figure 12: Thrust components in the arch along the nave. Constant basic friction coefficients.

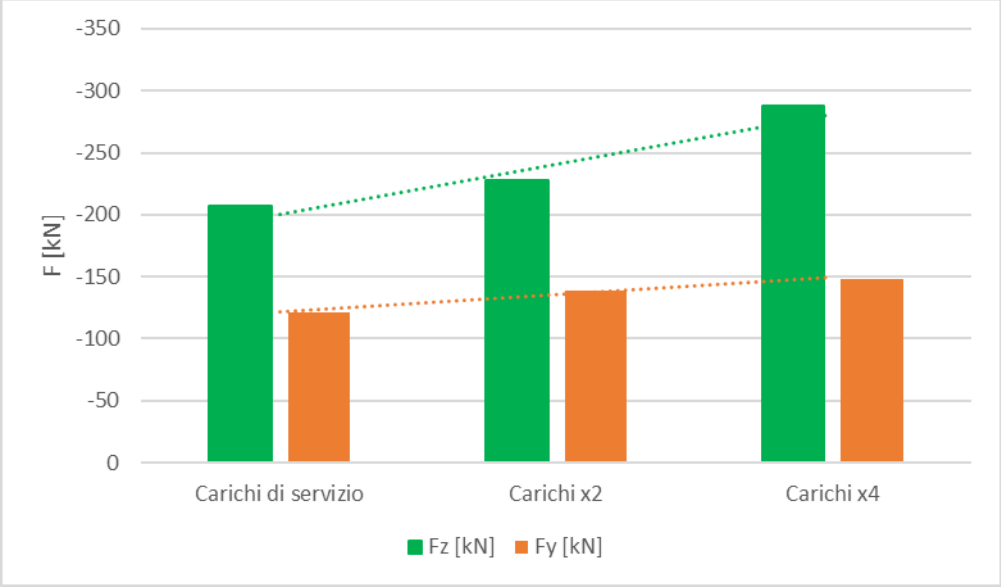

Figure 13: Thrust components in the arch along the transept. Constant basic friction coefficient.

The thrust components in the nave direction are greater than those in the transept direction because the arches along the nave cover a longer span. Moreover, both these components are much greater than the vertical components because exerted by lowered arches. Obviously, both horizontal and vertical components increase with increasing external loads. The load values obtained by multiplying by 2 the basic loads are very close to those indicated by the Technical Norms for incipient collapse (Ultimate Limit State - ULS). The resultant of the horizontal components corresponding to such loads is 400 kN approximately.

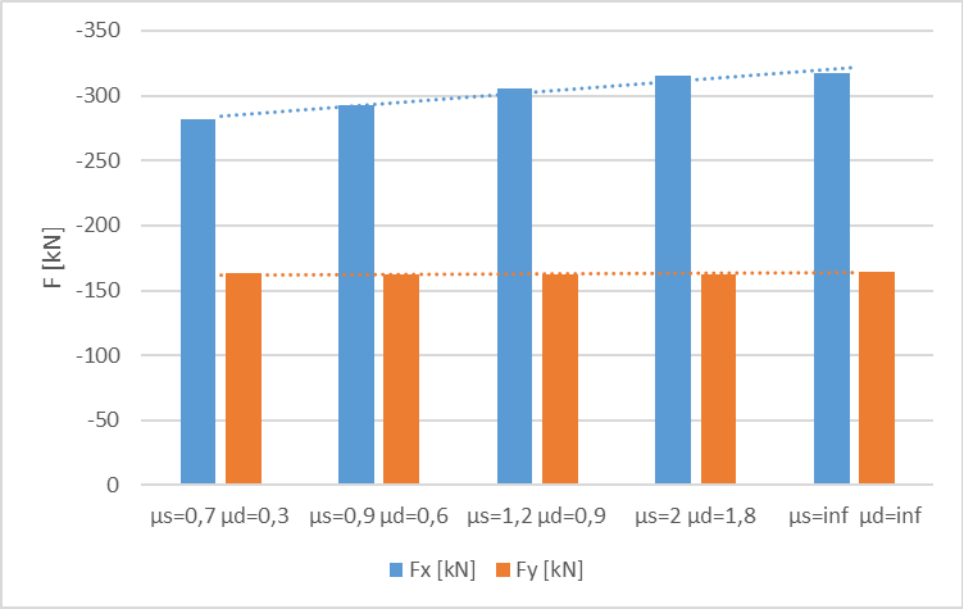

Figure 14: Thrust components in the arch along the nave. Constant basic loads.

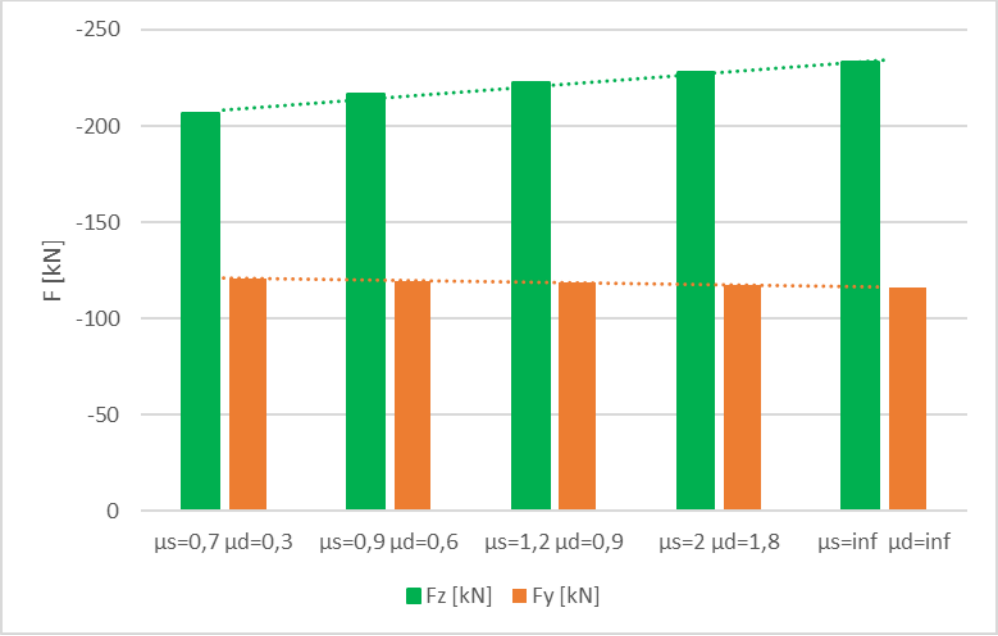

Figure 15: Thrust components in the arch along the transept. Constant basic loads.

Figure 15 and Figure 16 show the variation of the same components with increasing static and dynamic friction coefficients in the presence of constant basic loads. This analysis allows

to evaluate the sensitivity of the results to the changing of the friction coefficients up to an infinite value corresponding to a complete adherence or to an interpenetration at the interfaces.

As is obvious, the horizontal thrust components increase with increasing values of the friction coefficients, whereas the vertical components remain constant.

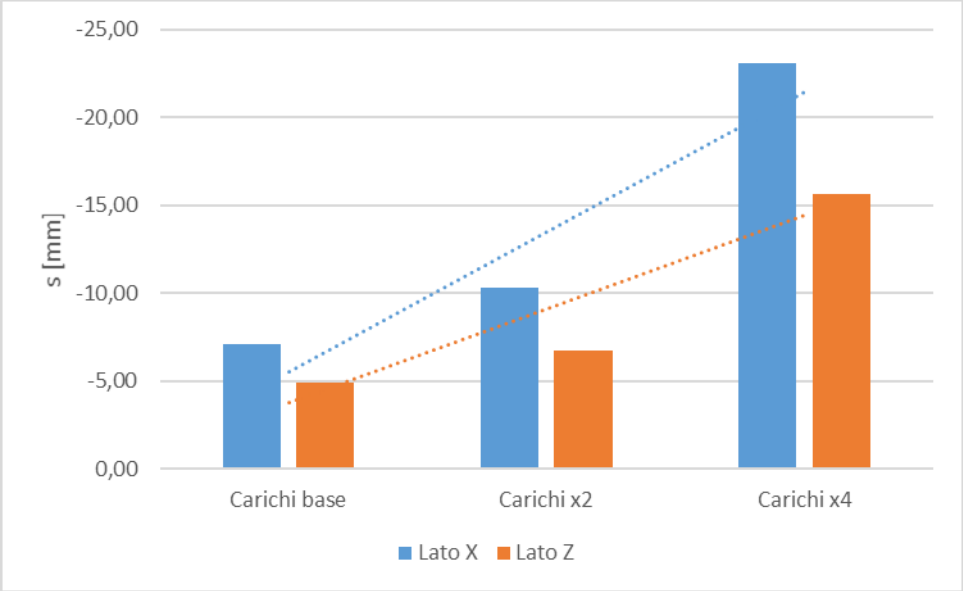

Figure 16: Maximum displacements with increasing loads and constant basic friction coefficients.

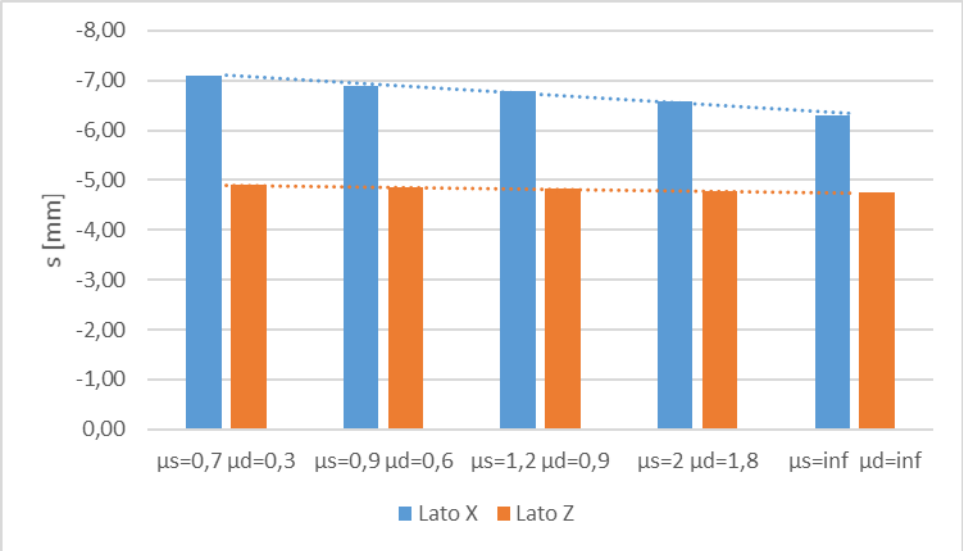

Figure 17: Maximum displacements with increasing friction coefficients and constant basic loads.

5.2 Maximum vertical displacements in the arches

In both arches the maximum vertical displacement (in the centreline) is computed in absence of filling between arches and lintels. This assumption can be justified, as mentioned before, by the presence of a low quality filling material which would not be able to contrast possible vertical displacements of the arch. As before, the analysis was carried out with constant basic friction coefficients and increasing loads and with constant basic loads and increasing friction coefficients (Figure 16 and Figure 17). "**s**" denotes the maximum vertical displacements in the arches in both X and Z directions, corresponding to nave and transept.

It is worth noting that these displacements vary considerably by increasing the loads, i.e from 5.4 mm to nearly 23 mm in the arch along the nave and from 5 mm to nearly 16 mm in the arch along the transept. Such values might seem too high at a first sight but they correspond to a progressive damage of the above masonry walls, as shown in the following Section. Moreover, they probably occurred in reality because of the low quality of the filling material between arch and lintel, as shown in Figure 18.

On the contrary, the increase of the friction coefficients causes a decrease of the maximum vertical displacements, as was expected, and this decrease is very small, less than 1 mm in the arch along the nave and nearly 0.1 mm in the arch along the transept.

Moreover, passing from the 2nd to the 3rd load condition the vertical displacement increases abruptly, more than the double in both nave and transept direction. That means that the 2nd load condition, or other load conditions between the 2nd and the 3rd, can be considered as corresponding to an incipient collapse. That also means that with these loads the masonry walls above the lintels undergo a considerable damage before finding a new state of equilibrium, as will be shown in the following.

Figure 18: Filling material between relieving arch and lintel.

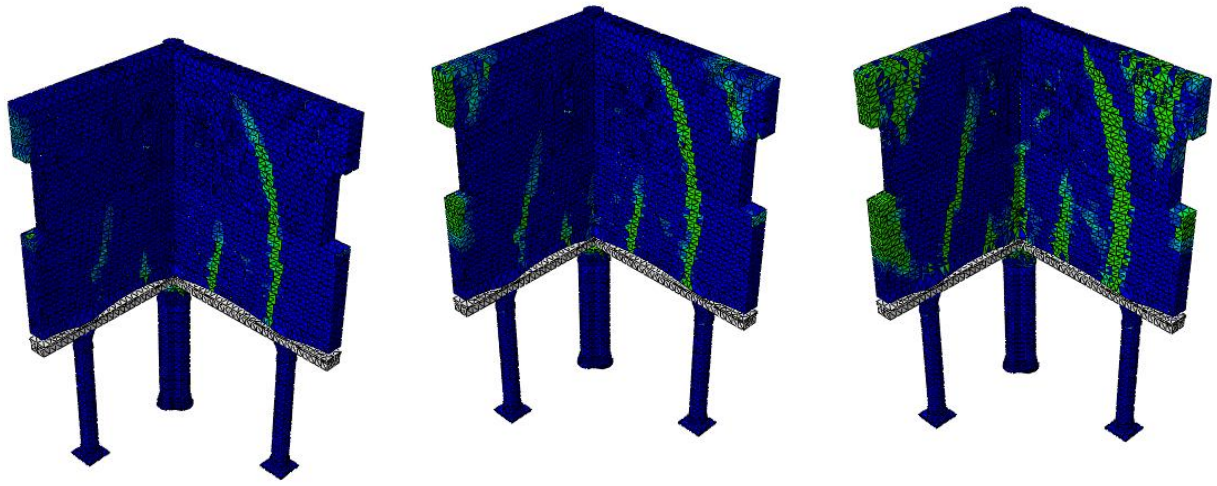

(a) (b) (c)

Figure 19: Crack pattern due to basic loads (a), multiplied by 2 (b) and by 4 (c).

5.3 Crack patterns

The *Concrete Damaged Plasticity* constitutive law chosen to model the material behaviour of masonry allows to identify the zones affected by damage due to tension and therefore by cracks. Although the crack pattern does not change considerably by increasing the friction coefficients (with constant basic loads), it changes a lot by increasing the loads (with constant basic friction coefficients), as shown in Figures 21, 22 and 23 where the different crack patterns are referred to the three load conditions used until now. It is worth noting that these crack patterns show a similarity: all the strips representing areas with lower strength or cracked areas start from the arches in proximity of the abutments and the key stones, where usually the hinges of the collapse mechanism occur (in arches with clamped of partially clamped extremities).

By increasing the loads these strips become more visible and move upwards, towards the top of the walls, up to join almost in correspondence of the common edge. It seems therefore that new relieving arches are formed in the walls above the actual ones so as to diminish the thrusts on the central column. Moreover, on the basis of such results, it can be supposed that the weight of the masonry enclosed between these new arches generated by the crack pattern and the lintels is transferred to the latter by the filling material.
Therefore, under this assumption, the lintels help to bear part of the vertical loads and the thrusts on the central column can be considered considerably reduced.

5.4 Analysis of the arch

An analysis of the arch in the nave direction (Figure 20) was carried out under incremental loads defined by means of λ multipliers with the aim of finding a relationship with the damage process analyzed in the previous Section.

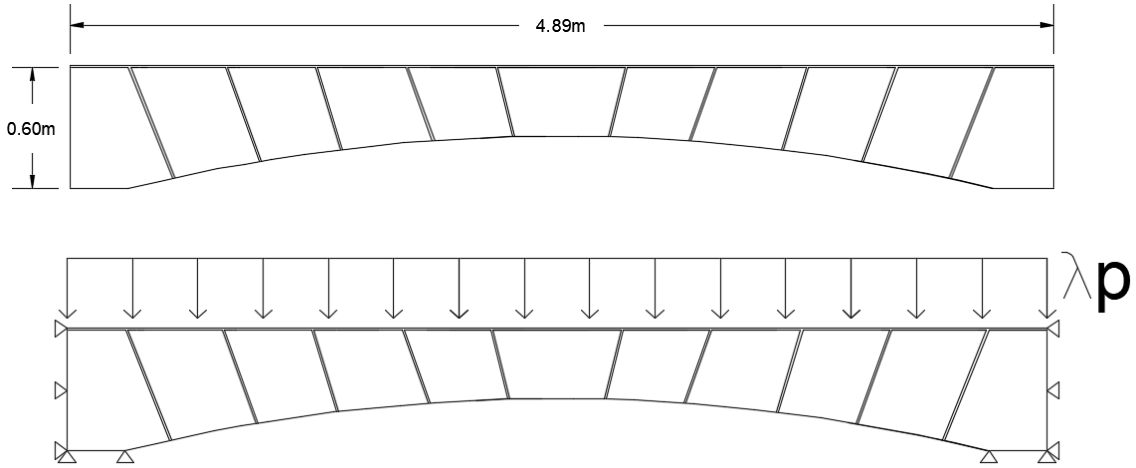

Figure 20: Geometric model of the arch and loading conditions.

The arch was modelled with plane strain shell elements with constant thickness equal to 59 cm, (stone thickness). Vertical and horizontal displacements are impeded at both horizontal and vertical extremities respectively; the arch is therefore clamped at both extremities. The load condition is given by a uniform incremental load with p=25000 N/m (Figure 20). The model is still heterogeneous and with the same mechanical characteristic as the global model.

The model was discretized with 1190 CPE4R plane strain elements with 4 nodes. In the mortar joints a finer mesh with 2 elements within the thickness was used in order to simulate better the behaviour of the mortar in tension up to the final collapse.

Table 8 contains the vertical displacements of the keystone of the arch in correspondence of increasing values of the λ multiplier. λ=4 provides the basic loads used in the previous Sections. Up to a λ value equal 10, far beyond the basic load condition, the vertical displacements increase linearly, i.e. the arch has a linear elastic behaviour. After this value the behaviour starts to be highly nonlinear as shown in Fig. 26.

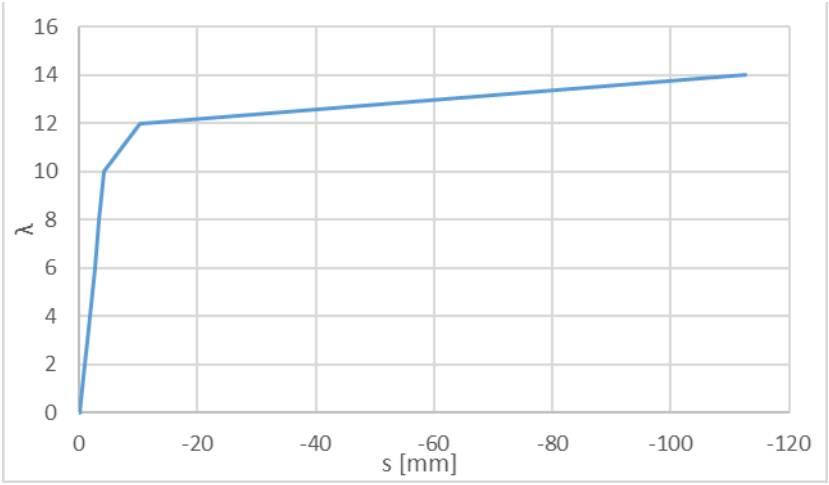

Figure 21: Vertical displacements vs multiplier λ.

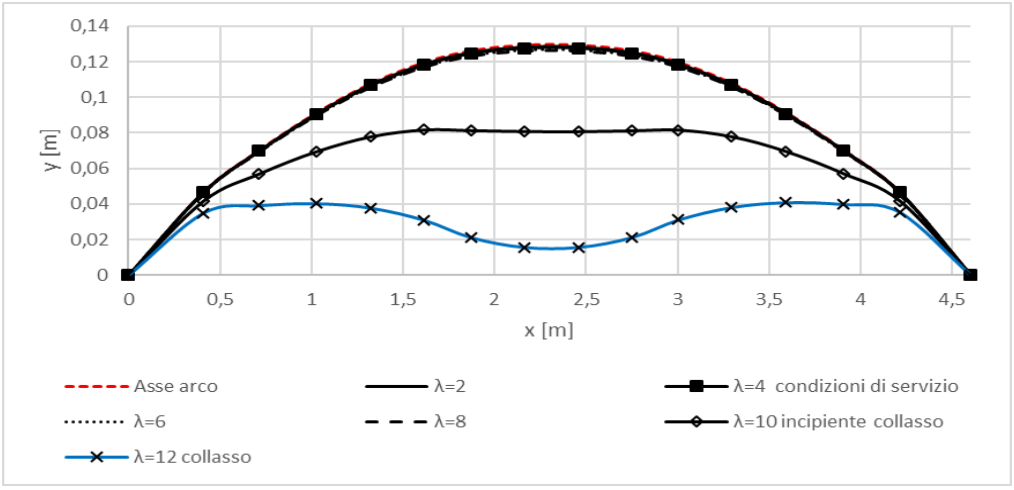

Figure 22: Deformed arch at variable values of λ multipliers

Figure 22 shows the deformation of the centre line of the arch at increasing values of the λ multipliers. For λ = 8, the double of the basic loads, i.e. the loads corresponding approximately to the Ultimate Limit State according to the Technical Norms, the arch is very close to the incipient collapse which occurs for λ=10 or for λ values slightly lower. It is worth noting that a displacement U=10 mm is here achieved for λ=12, far beyond the ULS load condition and when the clamped arch has already collapsed, whereas the same displacement in the global model with one sliding support and basic friction coefficients is already achieved with loads approximately close to the ULS condition. Therefore, it is possible to state that with the 2nd load condition in the global model, i.e. loads multiplied by 2 and corresponding to the ULS

load condition, the arch has already collapsed and that justifies the occurrence of the crack pattern showed before in the masonry above.

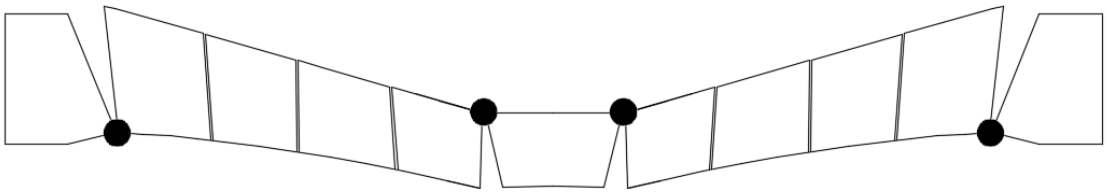

Figure 23: Collapse mechanism of the arch.

Figure 23 represents the collapse mechanism of the arch with the four hinges placed approximately where the cracks originate in the global model. The horizontal component of the thrust in the nave direction (Table 7) for λ=8 is more than the double of the same component in the global model with equivalent loads. But that is obvious because here both extremities are clamped. The lines of thrust at increasing values of λ (Figure 24) confirm the results shown before and in particular the collapse mechanism shown in Figure 25 for λ=12.

λ	Fx [kN]
2	-178.51
4	-344.60
6	-529.64
8	-772.13
10	-1125.65
12	-894.64

Table 7: Horizontal components of the thrust in the nave direction at variable values of λ multipliers.

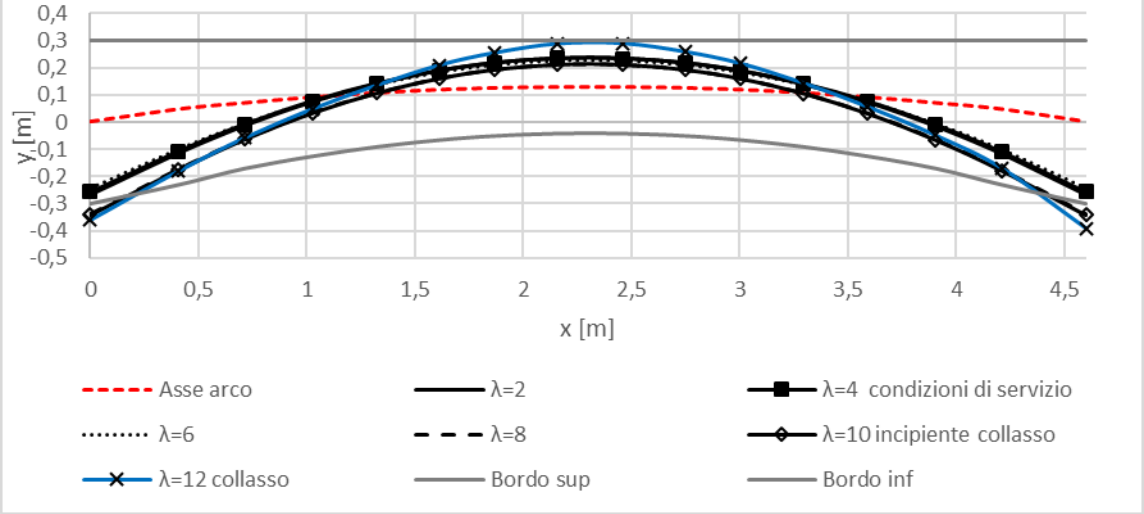

Figure 24: Lines of thrust for variable λ.

5.5 Analysis of the central column

The central column (Figure 26) has a bigger cross section than other columns because is subject to the thrusts coming from the arches of nave and transept. The analysis carried out in the global model with basic friction coefficients and basic loads shows that the column,

clamped at the basis, has a rotation towards the interior of the church whereas its capital has an opposite rotation. Therefore, the top of the column moves towards the interior, approximately in the direction of the resultant thrust, as shown in Figure 27 where the displacements (mm) in X and Y direction are represented with an amplification factor equal to 10. The same trend can be obtained also with increased values of loads and friction coefficients.

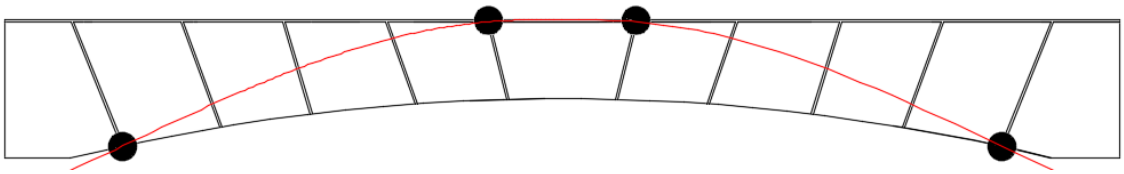

Figure 25: Line of thrust for λ=12 in the collapsed arch.

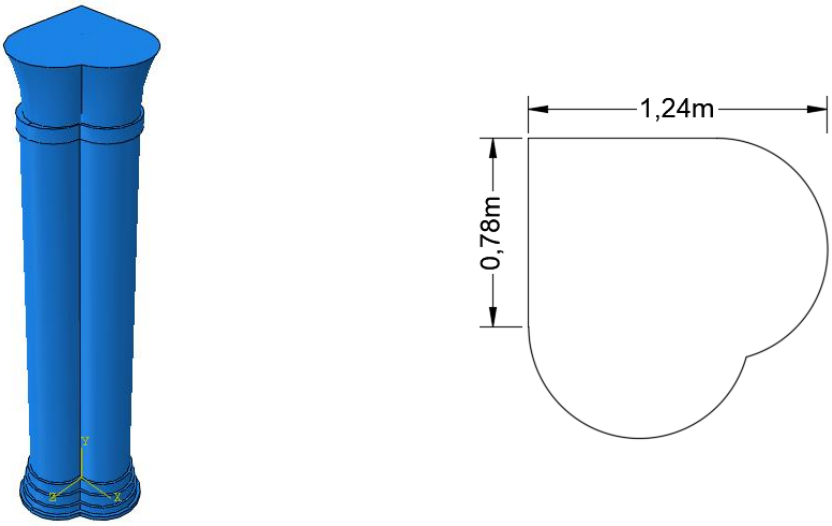

Figure 26: Central column of the corner.

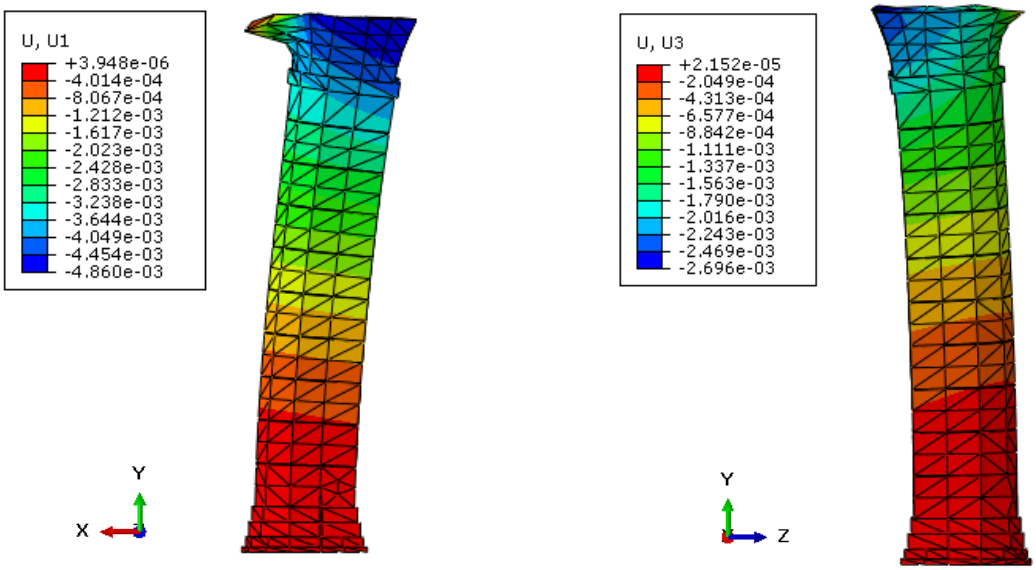

Figure 27: Displacements (mm) in X and Z direction of the central column.

Figure 28 shows the resultant displacements of the vertical axis of the column obtained by the composition of X and Z displacement components and referred to basic friction coefficients and increasing loads.

It is worth noting that for loads multiplied by 2, i.e. ULS load condition, the resultant horizontal displacement on the top of the column is just over 5 mm, whereas it increases considerably for grater loads. On the contrary, such displacements do not change a lot with increasing values of the friction coefficients, as shown in Figure 29 where the resultant horizontal displacements are computed for constant basic load conditions and variable friction coefficients. The difference between the maximum displacements referred to basic friction and infinite friction is less than 1 mm. It means that the particular conditions at the interfaces do not affect considerably the behaviour of the column and that, in the end, the maximum horizontal displacements of the column are contained within a very small range of values.

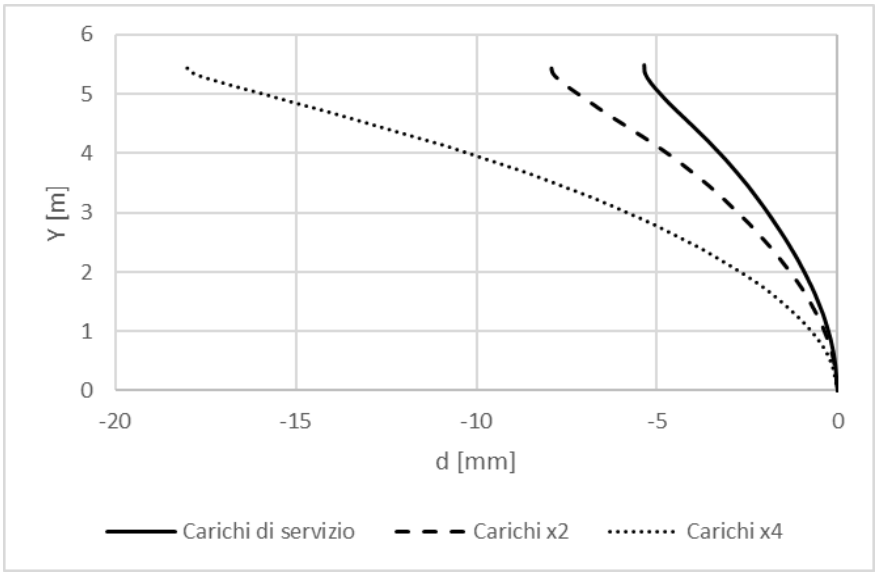

Figure 28: Resultant horizontal displacements along the axis of the column.

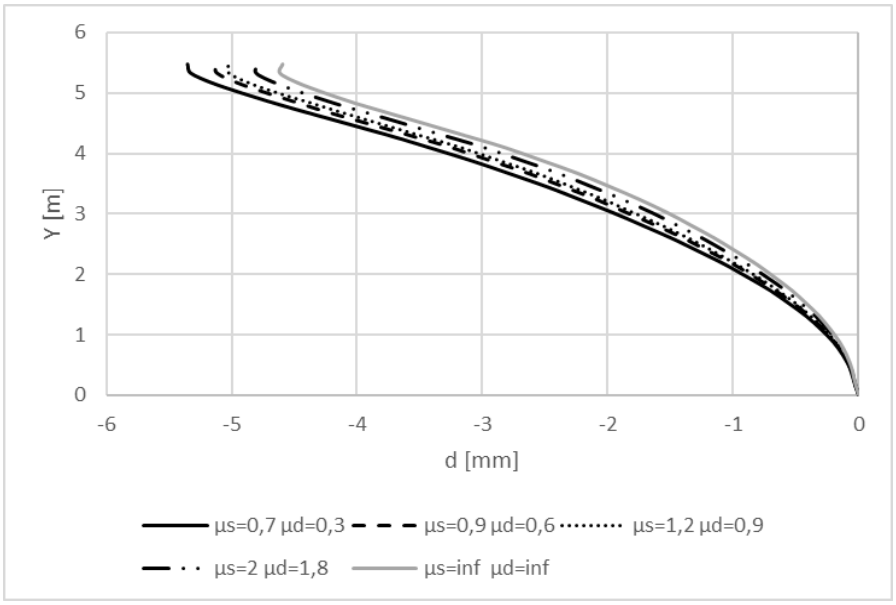

Figure 29: Resultant horizontal displacements with basic loads and variable friction coefficients.

As the damaged areas in the column, provided by the Damage Index in Tension, cannot be identified by using the global model and the corresponding discretization, the single column was analysed by using a new and finer mesh with a characteristic dimension equal to 5. Significant damages occur in the lowest part of the column only with loads multiplied by 2. This damage increases by incrementing the loads but it remains always in the lowest part of the column (Figure 30). On the contrary, some planes of weakness, although they cannot be considered yet as actual cracks, are actually present in other parts of the columns. Therefore, they might be independent of the particular state of stress and strain of the column and due to some initial defects or damages caused by past earthquakes.

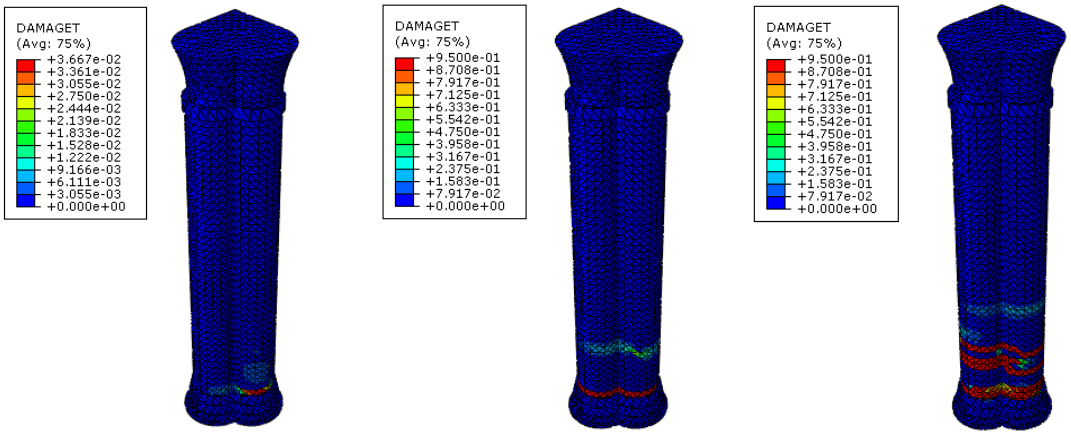

Figure 30: Damage Index in Tension with increasing loads (basic loads, loads multiplied by 2, loads multiplied by 4).

6 CONCLUSIONS

The two corners of the Church of the Nativity, the so called Armenian (North) and Orthodox corner (South), with reference to the two Religious Communities responsible for their maintenance according to the *status quo*, are still an unsolved problem which requires more onsite investigations and further numerical simulations.

In both corners the resultant of the horizontal components of the two thrusts coming from the relieving arches is transferred to the wooden lintels by friction, as no particular connection, like nails or iron rods, was found between masonry and lintels. Initial approximate calculations made with linear elastic models and with vertical loads corresponding, according with the Technical Norms, to the Ultimate Limit State (ULS) condition, provided resultant horizontal thrusts on both columns particularly high, far beyond the maximum values that can be transferred by the standard static and dynamic friction defined for the materials in contact. Nevertheless, despite some weakness planes surveyed in these columns, there are no signs of incipient collapse and both corners seem to be quite stable.

The aim of this paper was to provide a first explanation to this apparent paradox by using a FEM heterogeneous model implemented in Abaqus with increasing vertical loads and different friction coefficients. That allowed to understand the evolution of the damage in the masonry walls and in the columns in relation to various load and boundary conditions. In particular, a crack pattern in the walls is provided by the Damage Index in Tension by using basic (standard) friction coefficients and load conditions (basic loads multiplied by 2) approximately equal to those corresponding to the ULS condition prescribed by the Technical Norms at safety limit. This crack pattern shows the occurrence of crack lines starting from the arches and moving upwards so as to form new and higher relieving arches the thrusts of which on the

central columns become much lower than those computed with a linear elastic model. Moreover, the weight of that part of masonry contained between these arches and the lintels is borne by the lintels that, therefore, are not subject to tension only but also to vertical loads and bending moments. Such results are also confirmed by the analysis of the single arch subject to increasing vertical loads and clamped at both edges. The deformation of the central columns under the vertical loads and the thrusts transferred by friction by the relieving arches does not produce significant horizontal displacements such as to endanger their stability.

In conclusion, both corners can be still considered stable by virtue of the new resistant structure occurring within the walls but they are very near the state of incipient collapse if a ULS load conditions are considered. Moreover, as Bethlehem is in a seismic area, also a dynamic analysis should be carried out and probably the additional seismic actions might endanger the stability of the corners.

ACKNOWLEDGMENTS

The Authors are grateful to the Palestinian Presidential Committee, responsible for the restoration works in the Church of the Nativity, for authorizing in-depth studies on some still unsolved structural problems regarding the Church. They are also grateful to Eng. Maurizio Martinelli of the Piacenti s.r.l. technical staff for his precious and useful advices.

REFERENCES

[1] M. Bacci, G. Bianchi, S. Campana, G. Fichera, Historical and archaeological analysis of the Church of the Nativity. *Journal of Cultural Heritag*e, Special Issue, C. Alessandri ed., **13**(45), e1-e22, 2012.

[2] R.W. Hamilton, *The Church of the Nativity, Bethlehem, A Guide*, Jerusalem, 1947.

[3] W. Harvey et *al., The Church of the Nativity at Bethlehem*, London, 1910.

[4] B. Bagatti, *Gli antichi edifici sacri di Betlemme*, Jerusalem, 1952.

[5] N. Macchioni, M. Brunetti, B. Pizzo, P. Burato, M. Nocetti, S. Palanti, The timber structures in the Church of the Nativity in Bethlehem: Typologies and diagnosis. *Journal of Cultural Heritage*, Special Issue, C. Alessandri ed., **13**(4), e1-e12, 2012.

[6] C. Alessandri (coordinator), *Final Report delivered to the State of Palestine*, 2011.

[7] C. Alessandri (Ed.), The Church of the Nativity in Bethlehem: An interdisciplinary approach to a knowledge-based restoration. *Journal of Cultural Heritage*, Special Issue, **13**(4), 2012.

[8] A. Borri, A. De Maria, Indice di Qualità Muraria (IQM): correlazione con le caratteristiche meccaniche e livelli di conoscenza. *Progettazione sismica,* **6**, 45-63, 2015.

[9] Technical report delivered by the technical staff of Piacenti s.r.l. in charge of the restoration works in the Church, 2015.

[10] Circolare 617/2009, *Istruzioni per l'applicazione delle nuove Norme Tecniche per le Costruzioni di cui al decreto ministeriale*, 14 Gennaio 2008.

[11] Decreto Ministeriale 14 gennaio 2008, *Norme Tecniche per le Costruzioni*.

[12] ABAQUS®, *Theory Manual, Version 6.14*.

[13] J. Lee, G.L. Fenves, Plastic-damage model for cyclic loading of concrete structures. *Journal of Engineering Mechanics*, **124**, 892-900, 1998.

[14] J. Lubliner, J. Oliver, S. Oller, E. Oñate, A plastic-damage model for concrete. *International Journal of Solids and Structures*, **25**, 299-326, 1989.

[15] G. Milani, M. Valente, Comparative pushover and limit analyses on seven masonry churches damaged by the 2012 Emilia-Romagna (Italy) seismic events: possibilities of non-linear Finite Elements compared with pre-assigned failure mechanisms. *Engineering Failure Analysis*, **47**, 129-161, 2015.

[16] G. Milani, M. Valente, Failure analysis of seven masonry churches severely damaged during the 2012 Emilia-Romagna (Italy) earthquake: non-linear dynamic analyses vs conventional static approaches. *Engineering Failure Analysis*, **54**, 13-56, 2015.

[17] M. Valente, G. Milani, Seismic assessment of historical masonry towers by means of simplified approaches and standard FEM. *Construction and Building Materials*, **108**, 74-104, 2016.

[18] M. Valente, G. Milani, Non-linear dynamic and static analyses on eight historical masonry towers in the North-East of Italy. *Engineering Structures*, **114**, 241-270, 2016.

[19] G. Milani, M. Valente, C. Alessandri, The narthex of the Church of the Nativity in Bethlehem: a non-linear finite element approach to predict the structural damage. *Computers & Structures*, In press, 2018. doi: 10.1016/j.compstruc.2017.03.010

[20] E. Bertolesi, G. Milani, F. Lopane, M. Acito, Augustus Bridge in Narni (Italy): Seismic vulnerability assessment of the still standing part, possible causes of collapse and importance of the Roman concrete infill in the seismic-resistant behavior. *International Journal of Architectural Heritage*, **11**(5), 717-746, 2017.

[21] S. Tiberti, M. Acito, G. Milani, Comprehensive FE numerical insight into Finale Emilia Castle behaviour under 2012 Emilia Romagna seismic sequence: damage causes and seismic vulnerability mitigation hypothesis. *Engineering Structures*, **117**, 397-421, 2016.

[22] M. Acito, M. Bocciarelli, C. Chesi, G. Milani, Collapse of the clock tower in Finale Emilia after the May 2012 Emilia Romagna earthquake sequence: Numerical insight. *Engineering Structures*, **72**, 70-91, 2014

[23] G. Milani, P.B. Lourenco, A. Tralli, Homogenised limit analysis of masonry walls, Part I: failure surfaces. *Computers & Structures*, **84**(3-4), 166-180, 2006.